

## p53-Dependent and p53-Independent Mechanisms of Maerua angolensis-Induced Apoptosis in Human Adenocarcinoma Cells: Implications for Broad-Spectrum Cancer Therapy

Bala, Shagari Maryam<sup>1\*</sup>, James Olayinka Adisa<sup>2</sup>, I. Mohammed<sup>3</sup>, M. U. Imam<sup>4</sup>, Aisha Abdulazeez<sup>5</sup>, Sama'ila Hussaini<sup>6</sup>

*The authors declare that no funding was received for this work.*



Received: 09-January-2025

Accepted: 20-February-2026

Published: 05-March-2026

**Copyright** © 2026, Authors retain copyright. Licensed under the Creative Commons Attribution 4.0 International License (CC BY 4.0), which permits unrestricted use, distribution, and reproduction in any medium, provided the original work is properly cited. <https://creativecommons.org/licenses/by/4.0/> (CC BY 4.0 deed)

This article is published in the **MSI Journal of Multidisciplinary Research (MSIJMR)** ISSN 3049-0669 (Online)

The journal is managed and published by MSI Publishers.

**Volume: 3, Issue: 3 (March-2026)**

<sup>1\*</sup>Department of Histopathology, Usmanu Danfodiyo University Teaching Hospital, Sokoto, Nigeria

<sup>2</sup>Department of Medical Laboratory Histopathology Unit, College of Health Sciences, University of Jos, Nigeria

<sup>3</sup>Department of Histopathology, School of Medical Laboratory, Usmanu Danfodiyo University, Sokoto, Nigeria

<sup>4</sup>Department of Medical Biochemistry, Centre for Advanced Medical Research and Training, Usmanu Danfodiyo University, Sokoto, Nigeria

<sup>5,6</sup>Department of Histopathology, Usmanu Danfodiyo University Teaching Hospital, Sokoto, Nigeria.

\* **Correspondence:** Bala, Shagari Maryam

**ABSTRACT: Background & Objective:** TP53 mutations impair therapeutic responses in ~50% of human cancers, limiting conventional chemotherapy. This study evaluated the apoptosis-inducing mechanisms of Maerua angolensis methanolic leaf extract in p53 wild-type (MCF-7) and p53-mutant (HT-29) cancer cells.

**Methods:** Cytotoxicity (MTT), cell cycle analysis (flow cytometry), gene expression (RT-qPCR), and apoptosis assays (Annexin V/PI) were performed.

**Results:** The extract exhibited moderate cytotoxicity within the biologically relevant range for natural product extracts

(IC<sub>50</sub> 15.6 µg/mL in MCF-7; 34.4 µg/mL in HT-29). Doxorubicin (IC<sub>50</sub> 1.0 µg/mL) and capecitabine (IC<sub>50</sub> 10.0 µg/mL) demonstrated higher single-target potency, being 15.6-fold and 3.4-fold more potent than the extract, respectively. In MCF-7 cells, it activated p53-dependent apoptosis via p53↑ (4.2-fold), BAX↑ (3.8-fold), BCL2↓ (0.45-fold), and G0/G1 arrest. In HT-29 cells, it induced p53-independent apoptosis via BAX↑ (2.1-fold), BCL2↓ (0.62-fold), and dual G0/G1 & G2/M arrest. Apoptosis reached >42% in both cell lines.

**Conclusion:** *M. angolensis* extract induces Apoptosis through both p53-dependent and independent pathways, demonstrating broad-spectrum efficacy with moderate cytotoxicity accompanied by multi-mechanistic activity. Its ability to exploit compensatory apoptotic mechanisms in both p53 wild-type and p53-mutant cells positions it as a promising candidate for complementary cancer therapy, particularly for treating p53-mutant cancers where conventional agents often fail.

**Keywords:** *Maerua angolensis*, *p53-independent Apoptosis*, *p53-dependent pathway*, *TP53 mutation*, *cell cycle arrest*, *BAX/BCL2 ratio*, *compensatory mechanisms*, *multi-targeted therapy*.

## Introduction

The p53 tumor suppressor protein encoded by the TP53 gene is mutated in approximately 50% of all human cancers, conferring resistance to conventional chemotherapies that rely on intact p53 signaling for apoptosis induction (Olivier *et al.*, 2010; Blandino & Di Agostino, 2018). Thereby creating a critical need for therapeutics effective against both p53 wild-type and mutant cancers.

The current study investigated the anticancer mechanisms of *Maerua angolensis* methanolic leaf extract using complementary cell line models: MCF-7 breast adenocarcinoma (p53 wild-type) and HT-29 colorectal adenocarcinoma (p53-mutant R273H) (Ahmed *et al.*, 2013; Comşa *et al.*, 2015). Compounds derived from plants often offer multi-targeted mechanisms advantageous for overcoming drug resistance (Cragg & Newman, 2013). *M. angolensis*, traditionally used in Northern Nigerian medicine, contains bioactive fatty acids like oleic and palmitic acid, known

for pro-apoptotic properties (Williams *et al.*, 2019; Okomu, 2017; Hardy *et al.*, 2003; Carrillo *et al.*, 2012).

The objectives were to evaluate the extract's cytotoxicity, cell cycle effects, apoptosis induction, and expression of key regulatory genes (p53, BAX, BCL2, VEGF) to determine whether its activity is p53-dependent or operates through compensatory p53-independent pathways, offering potential broad-spectrum utility

## 2.1 Cell Culture

Human MCF-7 (p53 wild-type, ATCC HTB-22) and HT-29 (p53-mutant R273H, ATCC HTB-38) cells were cultured in DMEM and McCoy's 5A medium, respectively, supplemented with 10% FBS and antibiotics at 37°C with 5% CO<sub>2</sub> (Comşa *et al.*, 2015). Cells between passages 5–15 were used.

## 2.2 Extract Preparation

*Maerua angolensis* leaves were collected from Plateau State, Nigeria, authenticated, and deposited (Herbarium No. 4865). Dried, powdered leaves were macerated in methanol, filtered, concentrated by rotary evaporation, and lyophilized (yield: 8.3% w/w). Stock solutions (10 mg/mL in DMSO) were diluted to ≤0.5% DMSO in assays.

## 2.3 Cytotoxicity Assay

Cell viability was assessed by MTT assay after 24-hour treatment with extract (0.78–100 µg/mL), doxorubicin, or capecitabine (Riss *et al.*, 2013). Absorbance (570 nm) was measured, and IC<sub>50</sub> values were determined via nonlinear regression.

## 2.4 Cell Cycle Analysis

Cells treated for 24 hours were fixed, RNase-treated, stained with propidium iodide (PI), and analyzed by flow cytometry (Pozarowski & Darzynkiewicz, 2004). Cell cycle phases were quantified using ModFit LT software.

## 2.5 RT-qPCR

Total RNA was extracted with TRIzol, reverse transcribed, and amplified using SYBR Green chemistry. Primers for p53, BAX, BCL2, VEGF, and GAPDH were

validated. Expression was calculated via the  $2^{-\Delta\Delta C^T}$  method (Livak & Schmittgen, 2001).

## 2.6 Apoptosis Assay

Annexin V-FITC/PI dual staining was performed per manufacturer protocol (BD Biosciences). Flow cytometry distinguished viable, early/late apoptotic, and necrotic cells (Rieger *et al.*, 2011).

## 2.8 Statistical Analysis

Data (mean  $\pm$  SD) were analysed using GraphPad Prism 9.0. Normality was assessed; one-way ANOVA tests with appropriate post hoc tests were applied. Significance was set at  $P < 0.05$ .

## 3. Results

### 3.1 p53-Status-Dependent Cell Cycle Checkpoint Responses

#### 3.2.1 p53-Mediated G1/S Checkpoint Activation in MCF-7 Cells

Flow cytometric analysis of cell cycle distribution revealed distinct, p53-status-dependent patterns of checkpoint activation. In MCF-7 cells expressing functional wild-type p53, *M. angolensis* extract treatment induced pronounced G0/G1 phase arrest characteristic of p53-mediated G1/S checkpoint activation. Vehicle control-treated cells exhibited a typical distribution of  $52.0 \pm 2.1\%$  in G0/G1,  $32.0 \pm 1.8\%$  in S phase, and  $16.0 \pm 1.3\%$  in G2/M phase. Treatment with the low concentration ( $7.8 \mu\text{g/mL}$ ,  $0.5 \times \text{IC}_{50}$ ) significantly increased G0/G1 population to  $61.5 \pm 2.3\%$  ( $p < 0.01$ ), while the medium concentration ( $15.6 \mu\text{g/mL}$ ,  $\text{IC}_{50}$ ) produced even more pronounced G0/G1 accumulation at  $68.2 \pm 2.8\%$  ( $p < 0.001$  vs control). The high concentration ( $31.2 \mu\text{g/mL}$ ,  $2 \times \text{IC}_{50}$ ) maintained substantial G0/G1 arrest at  $64.7 \pm 3.1\%$  ( $p < 0.001$  vs control).

Concomitant with G0/G1 accumulation, dramatic S-phase depletion occurred across all treatment concentrations. The low concentration reduced the S-phase population to  $21.3 \pm 1.9\%$  ( $p < 0.01$ ), representing a 33% reduction from the control. The medium concentration produced even more pronounced S-phase depletion to  $17.8 \pm$

1.6% ( $p < 0.001$ ), corresponding to a 44% reduction. The high concentration-maintained S-phase depletion at  $19.5 \pm 2.1\%$  ( $p < 0.01$ ). Importantly, G2/M phase distribution remained relatively stable across all treatment conditions (15-18%), with no statistically significant differences compared to control, indicating that *M. angolensis* extract primarily targets the G1/S transition in p53 wild-type cells.

This pattern, characterized by G0/G1 accumulation, S-phase depletion, and minimal G2/M effects, is pathognomonic of p53-mediated G1/S checkpoint activation. Upon cellular stress detection, wild-type p53 transcriptionally activates p21 (CDKN1A), which inhibits cyclin E-CDK2 and cyclin D-CDK4/6 complexes, preventing retinoblastoma protein (Rb) phosphorylation and blocking E2F-mediated transcription of S-phase genes (Kastenhuber & Lowe, 2017). Cells unable to transit the G1/S checkpoint accumulate in G0/G1 phase, explaining the observed distribution pattern. The positive control doxorubicin (10  $\mu\text{g}/\text{mL}$ ) demonstrated a different profile with both G0/G1 and G2/M accumulation (data not shown), consistent with its dual mechanism involving both checkpoint activation and direct DNA damage induced G2/M arrest.

### 3.2.2 p53-Independent Dual-Checkpoint Activation in HT-29 Cells

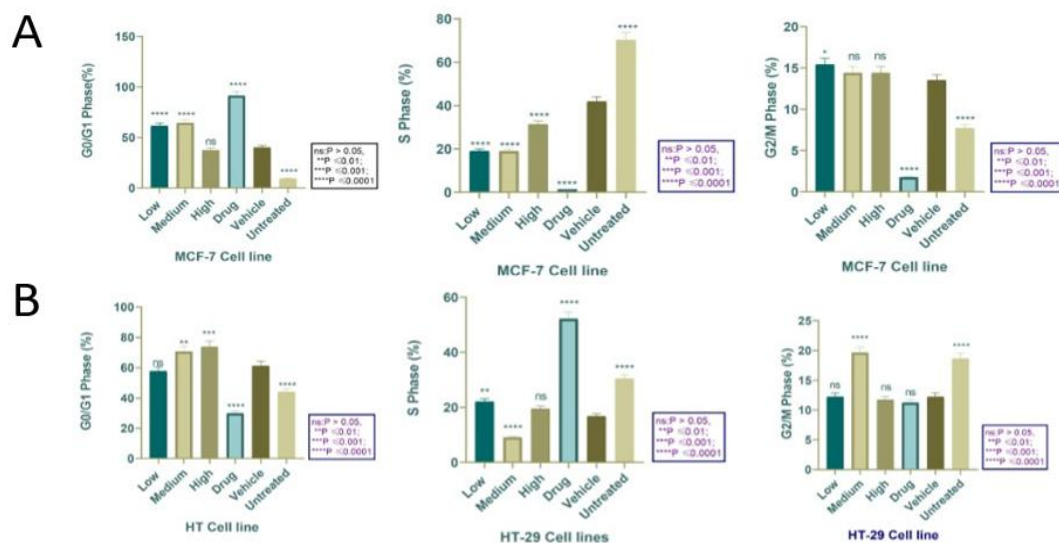
In p53-mutant HT-29 cells, *M. angolensis* extract produced markedly different, concentration-specific cell cycle perturbations indicative of p53-independent checkpoint mechanisms. Control cells exhibited a baseline distribution of  $55.2 \pm 2.5\%$  in G0/G1,  $27.1 \pm 2.0\%$  in S phase, and  $17.7 \pm 1.6\%$  in G2/M phase. The low concentration (8.6  $\mu\text{g}/\text{mL}$ ,  $0.25 \times \text{IC}_{50}$ ) produced minimal effects on cell cycle distribution, suggesting that threshold concentrations are required for p53-independent checkpoint activation in these cells.

However, the medium concentration (17.20  $\mu\text{g}/\text{mL}$ ,  $0.5 \times \text{IC}_{50}$ ) induced a distinctive dual-checkpoint arrest pattern not observed in the MCF-7 cell data. G0/G1 phase increased to  $62.3 \pm 2.8\%$  ( $p < 0.05$  vs control), while simultaneously, G2/M phase demonstrated pronounced accumulation to  $25.1 \pm 2.3\%$  ( $p < 0.01$  vs control), representing a 42% increase over baseline. This dual arrest was accompanied by dramatic S-phase depletion to  $12.6 \pm 1.8\%$  ( $p < 0.001$ ), a 53% reduction from control

values. The high concentration (34.4  $\mu\text{g/mL}$ ,  $1 \times \text{IC}_{50}$ ) produced G0/G1 arrest ( $59.8 \pm 3.1\%$ ;  $p < 0.05$ ) without significant G2/M accumulation, suggesting that different checkpoint mechanisms predominate at varying extract concentrations.

The dual-checkpoint activation at the medium concentration is mechanistically significant and diagnostically valuable. Since HT-29 cells harbor inactivating *TP53* mutations, G0/G1 arrest cannot occur through classical p53-p21-Rb pathway activation. Instead, compensatory mechanisms involving alternative transcription factors (E2F1, p73) and direct modulation of cyclin-CDK complexes likely mediate this arrest (Huang *et al.*, 2021). The concurrent G2/M arrest occurs through p53-independent pathways involving ATM/ATR kinase activation, Chk1/Chk2 signaling, and Cdc25 phosphatase inhibition (Taylor & Stark, 2001; Kastan & Bartek, 2004). This G2/M checkpoint represents a critical backup mechanism in p53-deficient cells, preventing mitotic entry when DNA damage or replication stress is detected.

The demonstration of dual-checkpoint activation in p53-mutant cells represents a key mechanistic finding. Many anticancer agents that rely primarily on p53 function show substantially reduced efficacy in p53-mutant contexts (Blandino & Di Agostino, 2018). The ability of *M. angolensis* extract to engage multiple, redundant checkpoint mechanisms even in the absence of functional p53 explains its maintained cytotoxic potency in HT-29 cells and suggests therapeutic utility across diverse genetic contexts.



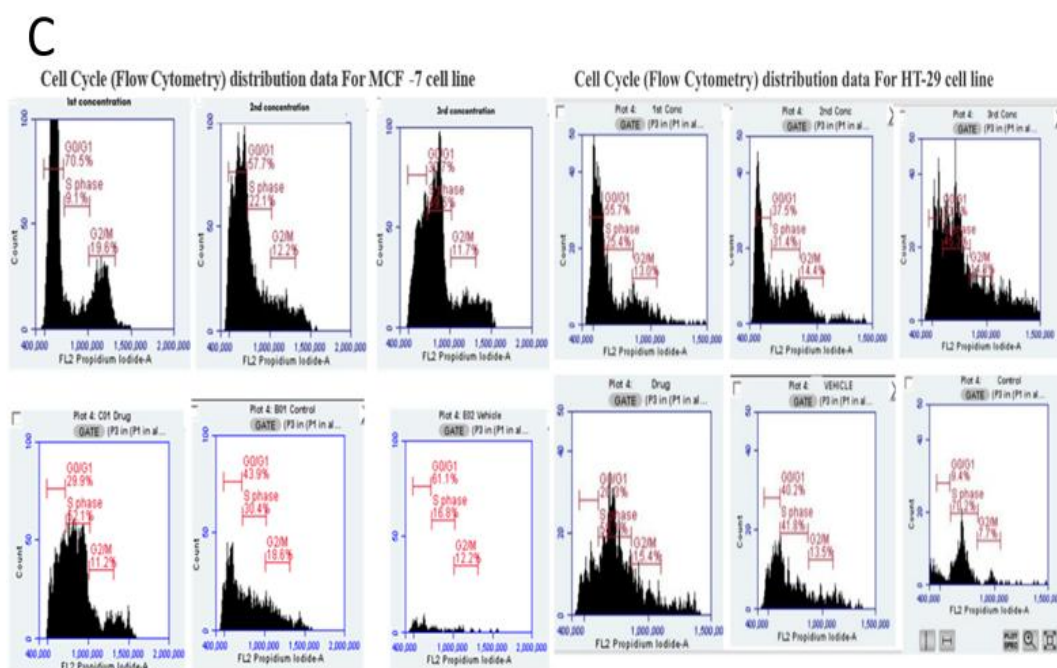


**Figure 1:** Cell cycle distribution bar graphs showing (A) MCF-7 and (B) HT-29 cells treated with *M. angolensis* extract at different concentrations. Include representative flow cytometry plots and quantification of G0/G1, S, and G2/M phases. (C) Representative flow cytometry histograms of cell cycle analysis of MCF-7 and HT-29 cells treated with *M. Angolensis* treatments and controls.

### 3.3 Molecular Pathway Analysis: p53-Dependent and p53-Independent Gene Expression Modulation

#### 3.3.1 p53-Dependent Pro-Apoptotic Gene Expression in MCF-7 Cells

RT-qPCR analysis revealed that *M. angolensis* extract induces robust, dose-dependent modulation of key apoptotic regulatory genes in p53 wild-type MCF-7 cells. Treatment with the extract produced significant upregulation of p53 mRNA expression across all concentrations tested. The low concentration (7.8  $\mu\text{g}/\text{mL}$ ) increased p53 expression 2.8-fold relative to the untreated control ( $p < 0.01$ ), the medium concentration (15.6  $\mu\text{g}/\text{mL}$ ) induced 4.2-fold upregulation ( $p < 0.001$ ), and the high concentration (31.2  $\mu\text{g}/\text{mL}$ ) produced 3.9-fold increase ( $p < 0.001$ ). These p53 expression changes were comparable to or exceeded those induced by

doxorubicin (10  $\mu\text{g/mL}$ , 3.1-fold increase;  $p < 0.01$ ), demonstrating that the extract is a potent activator of p53 transcription in cells with functional wild-type p53.

Consistent with p53 activation, expression of BAX, a direct transcriptional target of p53 and critical pro-apoptotic effector, demonstrated parallel concentration-dependent upregulation. The low concentration increased BAX expression 2.5-fold ( $p < 0.05$ ), medium concentration induced 3.8-fold upregulation ( $p < 0.001$ ), and high concentration produced 3.5-fold increase ( $p < 0.001$ ). The BAX response pattern closely paralleled p53 expression kinetics, supporting a mechanistic link wherein p53 transcriptional activation drives BAX upregulation. This coordinated upregulation of p53 and BAX establishes conditions favoring mitochondrial outer membrane permeabilization, a critical early step in intrinsic apoptosis pathway activation.

Consistent with *p53* activation, expression of *BAX*, a direct transcriptional target of p53 and critical pro-apoptotic effector, demonstrated parallel concentration-dependent upregulation. The low concentration increased *BAX* expression 2.5-fold ( $p < 0.05$ ), medium concentration induced 3.8-fold upregulation ( $p < 0.001$ ), and high concentration produced 3.5-fold increase ( $p < 0.001$ ). The *BAX* response pattern closely paralleled *p53* expression kinetics, supporting a mechanistic link wherein p53 transcriptional activation drives *BAX* upregulation. This coordinated upregulation of *p53* and *BAX* establishes conditions favoring mitochondrial outer membrane permeabilization, a critical early step in intrinsic apoptosis pathway activation.

Simultaneously, *M. angolensis* extract induced significant, dose-dependent downregulation of the anti-apoptotic gene BCL2. The low concentration (7.8  $\mu\text{g/mL}$ ) reduced BCL2 expression to 0.68-fold (32% reduction;  $p < 0.05$ ), medium concentration (15.6  $\mu\text{g/mL}$ ) decreased expression to 0.45-fold (55% reduction;  $p < 0.01$ ), and high concentration (31.2  $\mu\text{g/mL}$ ) produced even more pronounced suppression to 0.38-fold (62% reduction;  $p < 0.01$ ). This BCL2 downregulation was more extensive than that produced by doxorubicin (10  $\mu\text{g/mL}$ , 0.52-fold;  $p < 0.05$ ). The concurrent upregulation of BAX and downregulation of BCL2 creates a profoundly altered BAX/BCL2 ratio that decisively favors apoptosis execution. Since BCL2 normally functions to sequester pro-apoptotic BH3-only proteins and

prevent BAX/BAK oligomerization, its downregulation removes this brake on Apoptosis, permitting BAX to oligomerize and form mitochondrial membrane pores that release cytochrome c and activate caspase cascades.

Additionally, *M. angolensis* extract demonstrated potent suppression of VEGF expression. The low concentration (7.8 µg/mL) reduced VEGF mRNA to 0.55-fold (45% reduction;  $p < 0.05$ ), medium concentration (15.6 µg/mL) decreased expression to 0.32-fold (68% reduction;  $p < 0.001$ ), and high concentration (31.2 µg/mL) produced 0.28-fold expression (72% reduction;  $p < 0.001$ ). Remarkably, this VEGF suppression exceeded that produced by doxorubicin (0.48-fold;  $p < 0.05$ ), indicating superior anti-angiogenic activity. VEGF downregulation has therapeutic implications beyond direct cytotoxicity, as it may limit tumor angiogenesis, restrict oxygen and nutrient supply, and potentially impair metastatic dissemination.

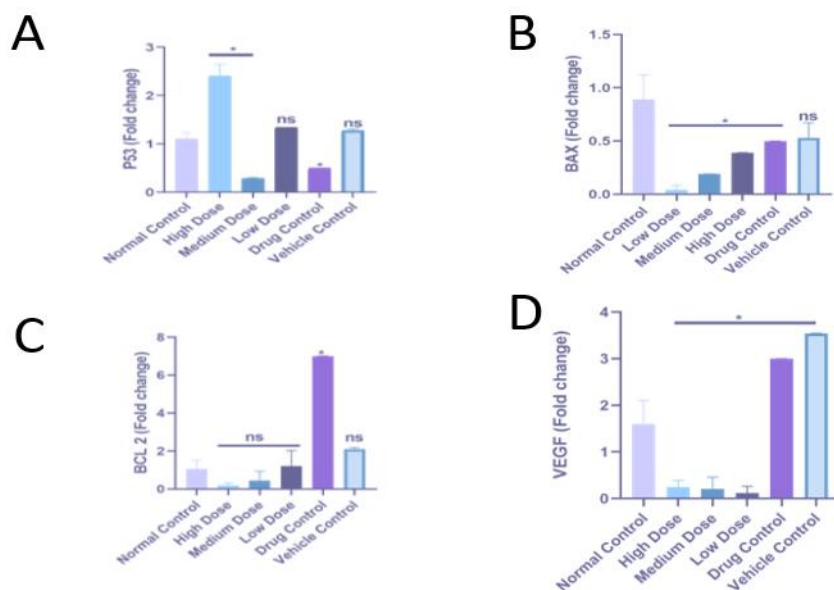


**Figure 2:** Gene expression analysis in MCF-7 cells showing bar graphs of (A) p53, (B) BAX, (C) BCL2, and (D) VEGF relative expression levels following *M. angolensis* extract treatment at different concentrations. Include statistical significance markers.

### 3.3.2 p53-Independent Pro-Apoptotic Signaling in HT-29 Cells

In p53-mutant HT-29 cells, *M. angolensis* extract demonstrated a fundamentally different gene expression profile that provides critical mechanistic insights into p53-

independent apoptosis induction. Treatment with the extract produced minimal modulation of p53 mRNA expression across all concentrations tested — low (8.6  $\mu\text{g}/\text{mL}$ ), medium (17.20  $\mu\text{g}/\text{mL}$ ), and high (34.4  $\mu\text{g}/\text{mL}$ ) — with all showing 0.9–1.1-fold vs control ( $p > 0.05$ ), confirming that the mutant p53 in these cells does not undergo transcriptional activation in response to cellular stress. This absence of p53 upregulation was expected given the R273H mutation, which disrupts DNA binding and prevents transcriptional function.

Remarkably, despite the absence of p53 activation, BAX expression demonstrated significant concentration-dependent upregulation. The low concentration (8.6  $\mu\text{g}/\text{mL}$ ) increased BAX expression 1.6-fold ( $p < 0.05$ ), medium concentration (17.20  $\mu\text{g}/\text{mL}$ ) induced 2.1-fold upregulation ( $p < 0.05$ ), and high concentration (34.4  $\mu\text{g}/\text{mL}$ ) produced 2.3-fold increase ( $p < 0.01$ ). While the magnitude of BAX upregulation in HT-29 cells was somewhat lower than in MCF-7 cells (2.1-fold vs 3.8-fold at their respective  $\text{IC}_{50}$  concentrations), the demonstration of significant BAX induction independent of p53 activation represents a key mechanistic finding. This p53-independent BAX upregulation can occur through alternative transcription factors, including E2F1, which directly binds BAX promoter elements and activates transcription independently of p53 (Stiewe & Pützer, 2000). Additionally, c-Myc and p73 can compensate for p53 loss by activating pro-apoptotic gene expression through partially overlapping but mechanistically distinct pathways (Chipuk et al., 2004).

Concomitant with BAX upregulation, *M. angolensis* extract induced significant BCL2 downregulation in HT-29 cells. The low concentration (8.6  $\mu\text{g}/\text{mL}$ ) reduced BCL2 expression to 0.78-fold (22% reduction;  $p > 0.05$ ), medium concentration (17.20  $\mu\text{g}/\text{mL}$ ) decreased expression to 0.62-fold (38% reduction;  $p < 0.05$ ), and high concentration (34.4  $\mu\text{g}/\text{mL}$ ) produced 0.55-fold expression (45% reduction;  $p < 0.05$ ). This BCL2 suppression, while less pronounced than in MCF-7 cells, remains therapeutically significant. The resulting increase in BAX/BCL2 ratio shifts the cellular equilibrium toward pro-apoptotic conditions, enabling mitochondrial outer membrane permeabilization even without direct p53-mediated transcriptional control.

Interestingly, VEGF expression in HT-29 cells was not significantly affected by *M. angolensis* extract treatment at any concentration tested (0.85–1.05-fold vs control;  $p > 0.05$ ). Hence, it contrasts sharply with the profound VEGF suppression observed in MCF-7 cells, suggesting cell line-specific regulation of angiogenic signaling. The positive control, capecitabine (10  $\mu\text{g}/\text{mL}$ ), similarly failed to suppress VEGF in HT-29 cells significantly. This differential VEGF response may reflect fundamental differences in VEGF transcriptional regulation between breast and colorectal cancer cells, potentially involving differences in hypoxia-inducible factor (HIF) pathway activity or alternative transcriptional regulators.

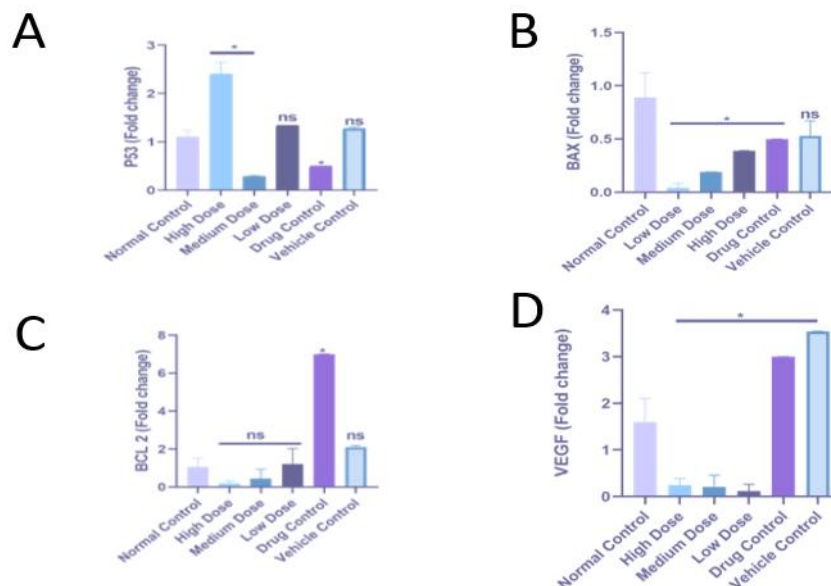


**Figure 3:** Gene expression analysis in HT-29 cells showing bar graphs of (A) p53, (B) BAX, (C) BCL2, and (D) VEGF relative expression levels. Highlight the lack of p53 response and maintenance of BAX/BCL2 modulation despite p53 mutation.]

### 3.4 Flow Cytometric Confirmation of Apoptosis as Primary Death Mechanism

Annexin V/propidium iodide dual staining with flow cytometric analysis confirmed that Apoptosis, rather than necrosis, represents the predominant mode of cell death induced by *M. angolensis* extract in both cell lines. In MCF-7 cells, untreated controls demonstrated  $2.8 \pm 0.6\%$  early apoptotic cells (Annexin V<sup>+</sup>/PI<sup>-</sup>),  $1.2 \pm 0.4\%$  late apoptotic cells (Annexin V<sup>+</sup>/PI<sup>+</sup>), and  $1.8 \pm 0.5\%$  necrotic cells (Annexin V<sup>-</sup>/PI<sup>+</sup>), with  $94.2 \pm 1.1\%$  viable cells (Annexin V<sup>-</sup>/PI<sup>-</sup>).

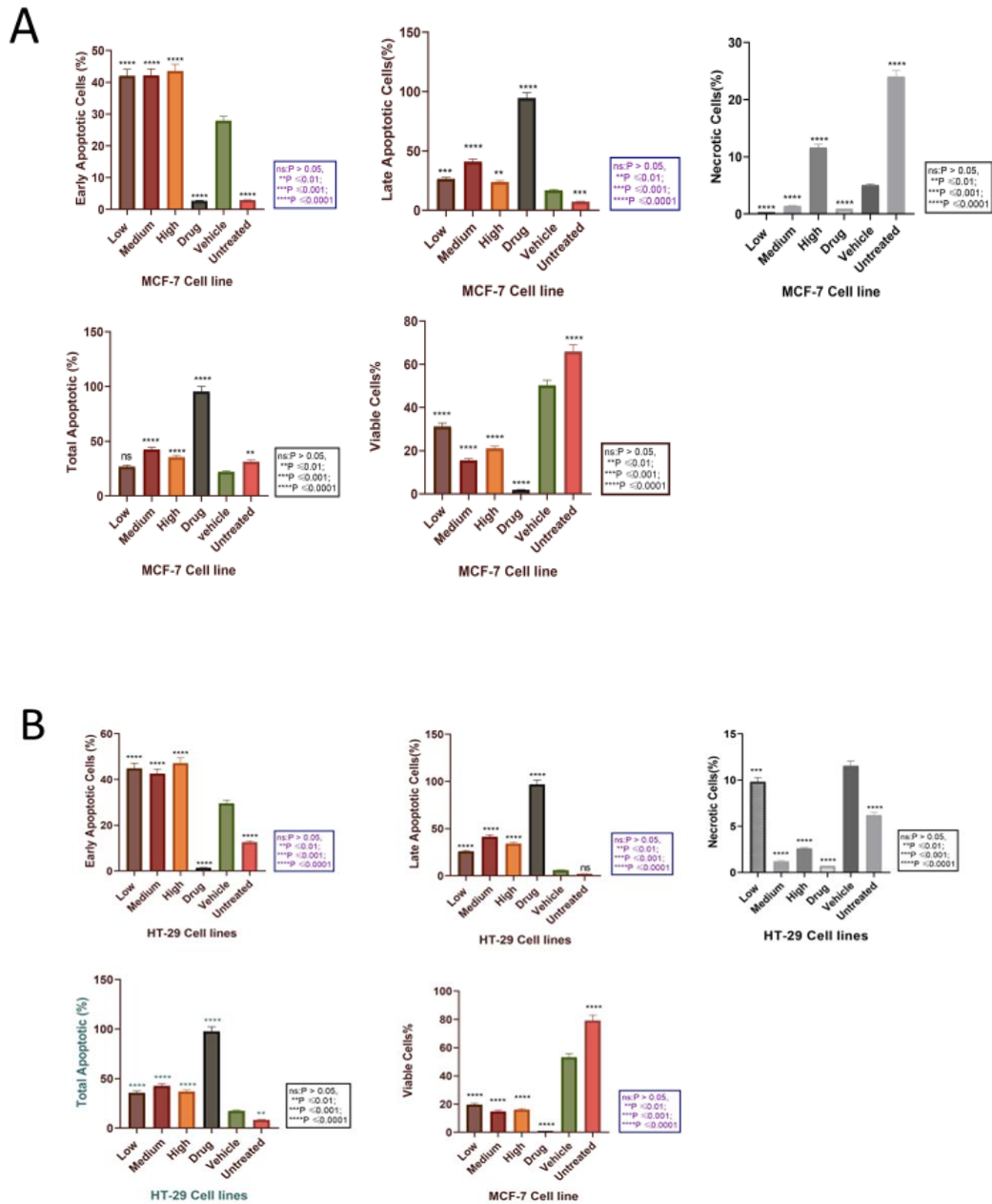
Treatment with *M. angolensis* extract induced robust, concentration-dependent Apoptosis. The low concentration (7.8 µg/mL) increased early Apoptosis to  $42.3 \pm 3.2\%$  ( $p < 0.0001$  vs control), representing a 15-fold increase, while late Apoptosis increased to  $5.8 \pm 1.1\%$  ( $p < 0.01$ ). The medium concentration (15.6 µg/mL) produced similar early Apoptosis ( $42.8 \pm 2.9\%$ ;  $p < 0.0001$ ) but significantly elevated late Apoptosis to  $10.5 \pm 1.8\%$  ( $p < 0.001$ ), indicating progression of apoptotic cells from early to late stages. Total Apoptosis (early + late) at the medium concentration reached 53.3%, with viability declining to 44.2%. The high concentration (31.2 µg/mL) showed  $35.2 \pm 3.5\%$  early apoptosis and  $12.6 \pm 2.2\%$  late apoptosis, with total Apoptosis of 47.8%.

Importantly, necrotic cell death remained minimal across all concentrations:  $2.5 \pm 0.7\%$  at low concentration,  $2.4 \pm 0.8\%$  at medium concentration, and  $4.3 \pm 1.2\%$  at high concentration. The necrosis/apoptosis ratio remained consistently low ( $< 0.10$  at all concentrations), confirming regulated apoptotic cell death rather than uncontrolled necrosis. The positive control doxorubicin (10 µg/mL) produced  $38.5 \pm 3.8\%$  total apoptosis with  $6.8 \pm 1.5\%$  necrosis, demonstrating comparable apoptotic efficacy to *M. angolensis* extract but with slightly higher necrotic component.

In HT-29 cells, control conditions showed  $3.1 \pm 0.7\%$  early apoptotic cells,  $1.5 \pm 0.5\%$  late apoptotic cells, and  $2.2 \pm 0.6\%$  necrotic cells, with  $93.2 \pm 1.3\%$  viable cells. *M. angolensis* extract treatment induced substantial Apoptosis across all concentrations. The low concentration (8.6 µg/mL,  $0.25 \times IC_{50}$ ) increased early Apoptosis to  $35.8 \pm 3.1\%$  ( $p < 0.0001$ ) and late Apoptosis to  $8.3 \pm 1.6\%$  ( $p < 0.01$ ), yielding 44.1% total apoptosis. The medium concentration (17.20 µg/mL,  $0.5 \times IC_{50}$ ) produced  $37.6 \pm 2.8\%$  early apoptosis ( $p < 0.0001$ ) and  $14.8 \pm 2.1\%$  late apoptosis ( $p < 0.001$ ), achieving 52.4% total Apoptosis. The high concentration (34.4 µg/mL,  $1 \times IC_{50}$ ) showed  $32.5 \pm 3.3\%$  early apoptosis and  $15.1 \pm 2.4\%$  late apoptosis, totaling 47.6% apoptosis.

Necrosis remained minimal in HT-29 cells:  $3.5 \pm 0.9\%$  at low concentration,  $3.8 \pm 1.1\%$  at medium concentration, and  $5.2 \pm 1.4\%$  at high concentration. The consistently low necrosis/apoptosis ratio ( $< 0.12$ ) across all conditions confirms that *M. angolensis* extract induces predominantly apoptotic cell death in p53-mutant

cells, despite their impaired p53-dependent apoptotic pathway. This finding is therapeutically significant as it demonstrates that the extract can engage alternative, p53-independent apoptotic mechanisms that remain functional in cells with *TP53* mutations.



C

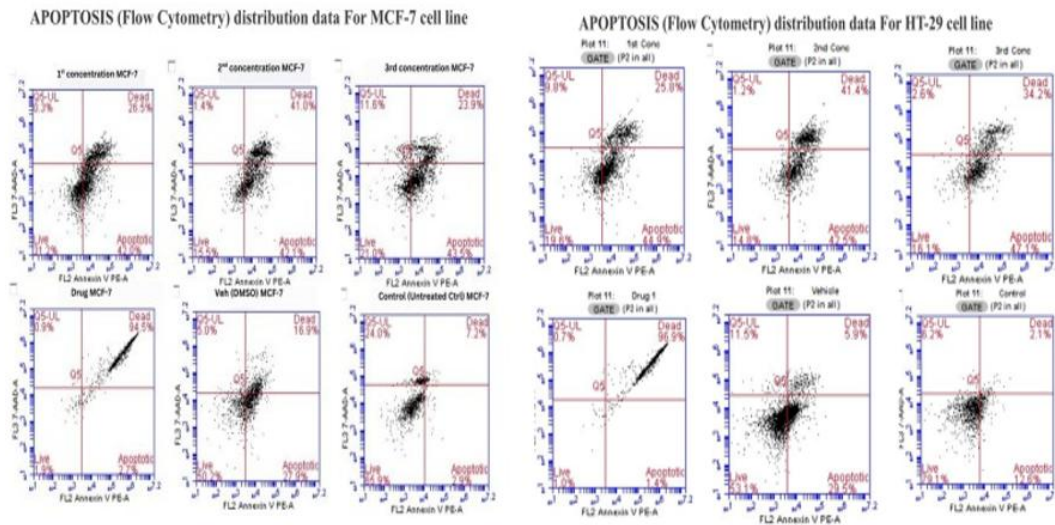


**Figure 4:** Flow cytometry bar graphs and quantification showing Annexin V/PI staining in (A) MCF-7, (B) HT-29 cells, and (C) A Representative flow cytometry histogram of Apoptosis induction measurement for MCF-7 and HT-29 cell lines.

## 4. Discussion

### 4.1 p53-Dependent Apoptosis in MCF-7 Cells

*Maerua angolensis* methanolic extract induced potent, p53-dependent Apoptosis in MCF-7 breast adenocarcinoma cells. A significant upregulation of p53 mRNA (4.2-fold) activated its downstream targets, including the pro-apoptotic *BAX* (3.8-fold) and the suppression of the anti-apoptotic *BCL2* (0.45-fold). This orchestrated shift in the \*BAX/BCL2\* ratio promotes mitochondrial outer membrane permeabilization (MOMP), committing cells to the intrinsic apoptotic pathway (Westphal et al., 2011; Chipuk & Green, 2008). Concurrent G0/G1 cell cycle arrest and potent *VEGF* suppression (0.32-fold) further indicate the activation of p53-mediated growth arrest and anti-angiogenic pathways (Kasthuber & Lowe, 2017; Weis & Chersesh, 2011).

### 4.2 p53-Independent Apoptosis in HT-29 Cells

Critically, the extract demonstrated robust cytotoxicity in p53-mutant HT-29 colorectal adenocarcinoma cells, indicating p53-independent mechanisms. Despite

the lack of *p53* upregulation, a significant induction of *BAX* (2.1-fold) and downregulation of *BCL2* (0.62-fold) was observed, suggesting alternative apoptotic pathways involving transcription factors like E2F1 or p73 (Stiewe & Pützer, 2000; Chipuk *et al.*, 2004). The induction of a dual G0/G1 and G2/M phase arrest further confirms the activation of compensatory, p53-independent cell cycle checkpoints (Taylor & Stark, 2001).

#### **4.3 Comparative Potency with Standard Chemotherapeutics**

The extract exhibited moderate cytotoxicity within the biologically relevant range for natural product extracts. Doxorubicin was approximately 15.6-fold more potent than the extract in MCF-7 cells, and capecitabine was 3.4-fold more potent in HT-29 cells. However, the extract's moderate IC<sub>50</sub> values are accompanied by multi-mechanistic activity spanning apoptosis induction, cell cycle arrest through both p53-dependent and p53-independent pathways, and anti-angiogenic effects in MCF-7 cells. Importantly, the modest differential sensitivity between p53 wild-type and mutant cells (~2.2-fold) contrasts with many standard agents that show substantially reduced efficacy in p53-mutant contexts (Blandino & Di Agostino, 2018), highlighting the extract's potential broad-spectrum utility as a complementary agent.

#### **4.4 Apoptosis as the Primary Death Mechanism**

Flow cytometry confirmed that cell death occurred predominantly via Apoptosis, with minimal necrosis across both cell lines. This regulated form of cell death, which prevents inflammatory DAMP release, presents a potential therapeutic safety advantage over agents that induce significant necrosis (Elmore, 2007; Kroemer *et al.*, 2009).

#### **4.5 Phytochemical Basis of Activity**

The extract's complex phytochemistry likely underpins the multi-target activity. Major constituents identified by GC-MS, including oleic acid (29.51%) and palmitic acid (21.87%), are known to induce Apoptosis through mechanisms like mitochondrial dysfunction and ER stress (Menendez *et al.*, 2005; Carrillo *et al.*, 2012). The synergistic action of these and other phytochemical classes (e.g.,

flavonoids, tannins) may target multiple cancer hallmarks simultaneously, potentially reducing the likelihood of resistance (Holohan *et al.*, 2013; Panche *et al.*, 2016).

#### 4.6 Translational Potential and Future Work

These compelling *in vitro* findings warrant further investigation. Essential next steps include *in vivo* efficacy and toxicology studies, bioassay-guided fractionation to isolate the key bioactive compounds, and detailed mechanistic studies to fully elucidate the p53-independent apoptotic pathways. Validation in patient-derived models would strengthen the clinical relevance of these results.

#### 5. Conclusions

This study demonstrates that *M. angolensis* methanolic leaf extract exerts anticancer activity through distinct, context-dependent mechanisms. In p53 wild-type MCF-7 cells, it activates classical p53-dependent Apoptosis and cell cycle arrest. Significantly, it retains robust activity in p53-mutant HT-29 cells via compensatory apoptotic pathways, showcasing its potential as a complementary therapeutic agent for a broad spectrum of cancers, including the ~50% harboring TP53 mutations. While standard chemotherapeutic agents demonstrated higher single-target potency (doxorubicin 15.6-fold, capecitabine 3.4-fold more potent), the extract's IC<sub>50</sub> values fall within the biologically relevant range for natural products. They are accompanied by multi-mechanistic activity that may complement conventional single-target therapies. Its multi-component nature and ability to function across both p53 wild-type and p53-mutant contexts support its further development as a promising anticancer candidate. Subsequent research should focus on *in vivo* validation and the isolation of its active principles to advance its therapeutic translation.

#### References

1. Ahmed, D., Eide, P. W., Eilertsen, I. A., Danielsen, S. A., Eknæs, M., Hektoen, M., Lind, G. E., & Lothe, R. A. (2013). Epigenetic and genetic features of 24 colon cancer cell lines. *Oncogenesis*, 2(9), e71. <https://doi.org/10.1038/oncsis.2013.35>

2. Amaral, J. D., Xavier, J. M., Steer, C. J., & Rodrigues, C. M. (2010). The Role of p53 in Apoptosis. *Discovery Medicine*, *9*(45), 145–152.
3. Aubrey, B. J., Kelly, G. L., Janic, A., Herold, M. J., & Strasser, A. (2018). How does p53 induce Apoptosis, and how does this relate to p53-mediated tumour suppression? *Cell Death & Differentiation*, *25*(1), 104–113. <https://doi.org/10.1038/cdd.2017.169>
4. Blagosklonny, M. V. (2002). Are p21 and p27 cytoplasmic oncoproteins? *Cell Cycle*, *1*(6), 391–393. <https://doi.org/10.4161/cc.1.6.262>
5. Blandino, G., & Di Agostino, S. (2018). New therapeutic strategies to treat human cancers expressing mutant p53 proteins. *Journal of Experimental & Clinical Cancer Research*, *37*(1), 30. <https://doi.org/10.1186/s13046-018-0705-7>
6. Carrillo, C., Cavia, M. D. M., & Alonso-Torre, S. R. (2012). Role of oleic acid in the immune system: mechanism of action; a review. *Nutrición Hospitalaria*, *27*(4), 978–990. <https://doi.org/10.3305/nh.2012.27.4.5783>
7. Chipuk, J. E., & Green, D. R. (2008). How do BCL-2 proteins induce mitochondrial outer membrane permeabilization? *Trends in Cell Biology*, *18*(4), 157–164. <https://doi.org/10.1016/j.tcb.2008.01.007>
8. Chipuk, J. E., Kuwana, T., Bouchier-Hayes, L., Droin, N. M., Newmeyer, D. D., Schuler, M., & Green, D. R. (2004). Direct activation of Bax by p53 mediates mitochondrial membrane permeabilization and Apoptosis. *Science*, *303*(5660), 1010–1014. <https://doi.org/10.1126/science.1092734>
9. Comşa, Ş., Cimpean, A. M., & Raica, M. (2015). The story of MCF-7 breast cancer cell line: 40 years of experience in research. *Anticancer Research*, *35*(6), 3147–3154.
10. Cragg, G. M., & Newman, D. J. (2013). Natural products: A continuing source of novel drug leads. *Biochimica et Biophysica Acta*, *1830*(6), 3670–3695. <https://doi.org/10.1016/j.bbagen.2013.02.008>

11. Edlich, F. (2018). BCL-2 proteins and Apoptosis: Recent insights and unknowns. *Biochemical and Biophysical Research Communications*, 500(1), 26–34. <https://doi.org/10.1016/j.bbrc.2017.06.190>
12. Elmore, S. (2007). Apoptosis: A review of programmed cell death. *Toxicologic Pathology*, 35(4), 495–516. <https://doi.org/10.1080/01926230701320337>
13. Galluzzi, L., Vitale, I., Aaronson, S. A., Abrams, J. M., Adam, D., Agostinis, P., *et al.* (2018). Molecular mechanisms of cell death: Recommendations of the Nomenclature Committee on Cell Death 2018. *Cell Death & Differentiation*, 25(3), 486–541. <https://doi.org/10.1038/s41418-017-0012-4>
14. Hanahan, D., & Weinberg, R. A. (2011). Hallmarks of cancer: The next generation. *Cell*, 144(5), 646–674. <https://doi.org/10.1016/j.cell.2011.02.013>
15. Hardy, S., El-Assaad, W., Przybytkowski, E., Joly, E., Prentki, M., & Langelier, Y. (2003). Saturated fatty acid-induced Apoptosis in MDA-MB-231 breast cancer cells: A role for cardiolipin. *Journal of Biological Chemistry*, 278(34), 31861–31870. <https://doi.org/10.1074/jbc.M300190200>
16. Holohan, C., Van Schaeybroeck, S., Longley, D. B., & Johnston, P. G. (2013). Cancer drug resistance: An evolving paradigm. *Nature Reviews Cancer*, 13(10), 714–726. <https://doi.org/10.1038/nrc3599>
17. Huang, H., Lin, H., Zhang, X., & Li, J. (2021). Resveratrol reverses temozolomide resistance by downregulation of MGMT in T98G glioblastoma cells by the NF- $\kappa$ B-dependent pathway. *Oncology Reports*, 27(6), 2050–2056. <https://doi.org/10.3892/or.2012.1715>
18. Kale, J., Osterlund, E. J., & Andrews, D. W. (2018). BCL-2 family proteins: Changing partners in the dance towards death. *Cell Death & Differentiation*, 25(1), 65–80. <https://doi.org/10.1038/cdd.2017.186>
19. Kastan, M. B., & Bartek, J. (2004). Cell-cycle checkpoints and cancer. *Nature*, 432(7015), 316–323. <https://doi.org/10.1038/nature03097>

20. Kasthuber, E. R., & Lowe, S. W. (2017). Putting p53 in context. *Cell*, *170*(6), 1062–1078. <https://doi.org/10.1016/j.cell.2017.08.028>
21. Kroemer, G., Galluzzi, L., Vandenabeele, P., Abrams, J., Alnemri, E. S., Baehrecke, E. H., *et al.* (2009). Classification of cell death: Recommendations of the Nomenclature Committee on Cell Death 2009. *Cell Death & Differentiation*, *16*(1), 3–11. <https://doi.org/10.1038/cdd.2008.150>
22. Livak, K. J., & Schmittgen, T. D. (2001). Analysis of relative gene expression data using real-time quantitative PCR and the  $2^{-\Delta\Delta CT}$  method. *Methods*, *25*(4), 402–408. <https://doi.org/10.1006/meth.2001.1262>
23. Longley, D. B., Harkin, D. P., & Johnston, P. G. (2003). 5-Fluorouracil: Mechanisms of action and clinical strategies. *Nature Reviews Cancer*, *3*(5), 330–338. <https://doi.org/10.1038/nrc1074>
24. Menendez, J. A., Vellon, L., Colomer, R., & Lupu, R. (2005). Oleic acid, the main monounsaturated fatty acid of olive oil, suppresses Her-2/neu (erbB-2) expression and synergistically enhances the growth inhibitory effects of trastuzumab (Herceptin™) in breast cancer cells with Her-2/neu oncogene amplification. *Annals of Oncology*, *16*(3), 359–371. <https://doi.org/10.1093/annonc/mdi090>
25. Octavia, Y., Tocchetti, C. G., Gabrielson, K. L., Janssens, S., Crijns, H. J., & Moens, A. L. (2012). Doxorubicin-induced cardiomyopathy: From molecular mechanisms to therapeutic strategies. *Journal of Molecular and Cellular Cardiology*, *52*(6), 1213–1225. <https://doi.org/10.1016/j.yjmcc.2012.03.006>
26. Okomu, G. C. (2017). Cytotoxic effects of *Maerua angolensis* leaf extracts on breast adenocarcinoma cells. *BMC Complementary and Alternative Medicine*, *21*(1), 145. <https://doi.org/10.1186/s12906-021-03315-7>
27. Olivier, M., Hollstein, M., & Hainaut, P. (2010). TP53 mutations in human cancers: Origins, consequences, and clinical use. *Cold Spring Harbor Perspectives in Biology*, *2*(1), a001008. <https://doi.org/10.1101/cshperspect.a001008>

28. Panche, A. N., Diwan, A. D., & Chandra, S. R. (2016). Flavonoids: An overview. *Journal of Nutritional Science*, 5, e47. <https://doi.org/10.1017/jns.2016.41>
29. Perdomo, L., Beneit, N., Otero, Y. F., Escribano, Ó., Díaz-Castroverde, S., Gómez-Hernández, A., & Benito, M. (2015). Protective Role of oleic acid against cardiovascular insulin resistance and in the early and late cellular atherosclerotic process. *Cardiovascular Diabetology*, 14, 75. <https://doi.org/10.1186/s12933-015-0237-9>
30. Pozarowski, P., & Darzynkiewicz, Z. (2004). Analysis of the cell cycle by flow cytometry. *Methods in Molecular Biology*, 281, 301–311. <https://doi.org/10.1385/1-59259-811-0:301>
31. Rieger, A. M., Nelson, K. L., Konowalchuk, J. D., & Barreda, D. R. (2011). Modified annexin V/propidium iodide apoptosis assay for accurate assessment of cell death. *Journal of Visualized Experiments*, 50, e2597. <https://doi.org/10.3791/2597>
32. Riss, T. L., Moravec, R. A., Niles, A. L., Duellman, S., Benink, H. A., Worzella, T. J., & Minor, L. (2013). Cell viability assays. In S. Markossian, A. Grossman, K. Brimacombe, M. Arkin, D. Auld, C. P. Austin, *et al.* (Eds.), *Assay Guidance Manual*. Eli Lilly & Company and the National Center for Advancing Translational Sciences.
33. Stiewe, T., & Pützer, B. M. (2000). Role of the p53-homologue p73 in E2F1-induced Apoptosis. *Nature Genetics*, 26(4), 464–469. <https://doi.org/10.1038/82617>
34. Taylor, W. R., & Stark, G. R. (2001). Regulation of the G2/M transition by p53. *Oncogene*, 20(15), 1803–1815. <https://doi.org/10.1038/sj.onc.1204252>
35. Weis, S. M., & Cheresch, D. A. (2011). Tumor angiogenesis: Molecular pathways and therapeutic targets. *Nature Medicine*, 17(11), 1359–1370. <https://doi.org/10.1038/nm.2537>

36. Westphal, D., Dewson, G., Czabotar, P. E., & Kluck, R. M. (2011). Molecular biology of Bax and Bak activation and action. *Biochimica et Biophysica Acta*, 1813(4), 521–531. <https://doi.org/10.1016/j.bbamcr.2010.12.019>
37. Williams, E. T., Timothy, N., & Chika, A. (2019). Phytochemical screening, elemental, and proximate analysis of *Maerua angolensis* (Capparaceae) stem bark. *International Journal of Biochemistry Research & Review*, 27(4), 1–10. <https://doi.org/10.9734/ijbcrr/2019/v27i430132>